



## HUMAN & MOUSE CELL LINES

Engineered to study multiple immune signaling pathways.

Transcription Factor, PRR, Cytokine, Autophagy and COVID-19 Reporter Cells  
ADCC, ADCC and Immune Checkpoint Cellular Assays



# The Journal of Immunology

RESEARCH ARTICLE | OCTOBER 15 2002

## Comparison of the Pro-Oxidative and Proinflammatory Effects of Organic Diesel Exhaust Particle Chemicals in Bronchial Epithelial Cells and Macrophages<sup>1</sup> **FREE**

Ning Li; ... et. al

*J Immunol* (2002) 169 (8): 4531–4541.

<https://doi.org/10.4049/jimmunol.169.8.4531>

### Related Content

Diesel Exhaust Particle-Exposed Human Bronchial Epithelial Cells Induce Dendritic Cell Maturation

*J Immunol* (June,2006)

Thiol Antioxidants Inhibit the Adjuvant Effects of Aerosolized Diesel Exhaust Particles in a Murine Model for Ovalbumin Sensitization

*J Immunol* (March,2002)

MicroRNA-375 Regulation of Thymic Stromal Lymphopoietin by Diesel Exhaust Particles and Ambient Particulate Matter in Human Bronchial Epithelial Cells

*J Immunol* (April,2013)

# Comparison of the Pro-Oxidative and Proinflammatory Effects of Organic Diesel Exhaust Particle Chemicals in Bronchial Epithelial Cells and Macrophages<sup>1</sup>

Ning Li,\* Meiyang Wang,\* Terry D. Oberley,<sup>†</sup> Joan M. Sempf,<sup>‡</sup> and Andre E. Nel<sup>2\*</sup>

Inhaled diesel exhaust particles (DEP) exert proinflammatory effects in the respiratory tract. This effect is related to the particle content of redox cycling chemicals and is involved in the adjuvant effects of DEP in atopic sensitization. We demonstrate that organic chemicals extracted from DEP induce oxidative stress in normal and transformed bronchial epithelial cells, leading to the expression of heme oxygenase 1, activation of the c-Jun N-terminal kinase cascade, IL-8 production, as well as induction of cytotoxicity. Among these effects, heme oxygenase 1 expression is the most sensitive marker for oxidative stress, while c-Jun N-terminal kinase activation and induction of apoptosis-necrosis require incremental amounts of the organic chemicals and increased levels of oxidative stress. While a macrophage cell line (THP-1) responded in similar fashion, epithelial cells produced more superoxide radicals and were more susceptible to cytotoxic effects than macrophages. Cytotoxicity is the result of mitochondrial damage, which manifests as ultramicroscopic changes in organelle morphology, a decrease in the mitochondrial membrane potential, superoxide production, and ATP depletion. Epithelial cells also differ from macrophages in not being protected by a thiol antioxidant, *N*-acetylcysteine, which effectively protects macrophages against cytotoxic DEP chemicals. These findings show that epithelial cells exhibit a hierarchical oxidative stress response that differs from that of macrophages by more rapid transition from cytoprotective to cytotoxic responses. Moreover, epithelial cells are not able to convert *N*-acetylcysteine to cytoprotective glutathione. *The Journal of Immunology*, 2002, 169: 4531–4541.

Epidemiological studies have demonstrated an association between exposure to ambient particulate matter (PM)<sup>3</sup> and adverse cardiorespiratory effects (1–5). These adverse effects include an exacerbation of asthma and allergic inflammation (1–5). While there has been considerable debate about the contribution of particles vs chemical components (e.g., nitrates, sulfates, transition metals, and organic chemicals), our studies, using diesel exhaust particles (DEP) as a model air pollutant, have shown that organic chemical compounds play an important role in the pro-oxidative and proinflammatory effects of these particles in the respiratory tract (6–9). DEP have a mass medium diameter of 0.05–1  $\mu\text{m}$  (mean, 0.2  $\mu\text{m}$ ), a size that renders them easily respirable and capable of depositing in the airways and alveoli. DEP

consist of a carbonaceous core with a large surface area to which chemicals are absorbed. These include organic chemicals such as polycyclic aromatic hydrocarbons (PAH), nitro derivatives of PAH, oxygenated derivatives of PAH (ketones, quinones, and diones), heterocyclic compounds, aldehydes, and aliphatic hydrocarbons (10–14). Our interest lies with the PAH and their oxygenated derivatives (e.g., quinones), which are able to redox cycle and generate reactive oxygen species (ROS) in target cell populations such as macrophages (8, 14–19). The pro-oxidative effects of intact DEP or crude DEP extracts can be reproduced with fractionated aromatic and polar chemical groups, which are enriched for PAH and quinones, respectively (11–14, 20). Similarly, intact DEP or organic DEP extracts induce pro-oxidative and proinflammatory effects in the respiratory tract, which can be negated by thiol antioxidants (10, 16).

Macrophages constitute an important target for DEP in the lung (17, 18, 21–23). After phagocytosis of these particles, macrophages respond in a hierarchical fashion to increasing particle load and incremental levels of oxidative stress (24). Thus, at low oxidative stress levels, as defined by no or minimal change in the cellular reduced glutathione (GSH)/glutathione disulfide (GSSG) ratios, these cells mount antioxidant and cytoprotective responses, e.g., heme oxygenase 1 (HO-1) and superoxide dismutase expression (24). HO-1 expression is dependent on the function of antioxidant response element (ARE) in its promoter (11) and is typically induced by 1–10  $\mu\text{g}/\text{ml}$  of the DEP extract (11, 24). In contrast, extract doses of 10–50  $\mu\text{g}/\text{ml}$  are required to activate intracellular pathways, such as the c-Jun N-terminal kinase (JNK) and NF- $\kappa\text{B}$  cascades, which are responsible for proinflammatory effects (24). Activation of these cascades may constitute the principal mechanism by which DEP exert adjuvant effects in the lung (7, 8, 24). At even higher oxidative stress levels, which coincide with extract doses of >50  $\mu\text{g}/\text{ml}$ , macrophages undergo apoptosis and necrosis (17, 18, 24).

\*Division of Clinical Immunology and Allergy, Department of Medicine, University of California, Los Angeles, CA 90095; <sup>†</sup>Department of Pathology and Laboratory Medicine, University of Wisconsin, Madison, WI 53706; and <sup>‡</sup>Pathology Service, Veterans Affairs Medical Center, Madison, WI 53705

Received for publication May 15, 2002. Accepted for publication August 2, 2002.

The costs of publication of this article were defrayed in part by the payment of page charges. This article must therefore be hereby marked *advertisement* in accordance with 18 U.S.C. Section 1734 solely to indicate this fact.

<sup>1</sup> This work was supported by U.S. Public Health Service Grants AI50495 and ES10553.

<sup>2</sup> Address correspondence and reprint requests to Dr. Andre E. Nel, Division of Clinical Immunology and Allergy, Department of Medicine, University of California, 10833 Le Conte Avenue, 52-175 CHS, Los Angeles, CA 90095. E-mail address: anel@mednet.ucla.edu

<sup>3</sup> Abbreviations used in this paper: PM, particulate matter; ARE, antioxidant response element; BEGM, Bronchial epithelial growth medium; CoPP, cobalt protoporphyrin; DCF, dihydrochlorofluorescein diacetate; DEP, diesel exhaust particles; DiOC<sub>6</sub>, 3,3'-dihexyloxycarbocyanine iodide;  $\Delta\Psi\text{m}$ , mitochondrial membrane potential; GSH, reduced glutathione; GSSG, glutathione disulfide; HE, hydroethidine; HO-1, heme oxygenase-1; JNK, c-Jun N-terminal kinase; LL, lower left; MnSOD, manganese superoxide dismutase; NAC, *N*-acetylcysteine; NHBE, normal human bronchial epithelial cells; O<sub>2</sub><sup>-</sup>, superoxide radical; PAM, pulmonary alveolar macrophages; PI, propidium iodide; phospho-JNK, phosphorylated JNK; PT, permeability transition; ROS, reactive oxygen species; UL, upper left; UR, upper right.

Bronchial epithelial cells are another primary cell target for PM (25–28). Not only do these cells play an important role in allergic inflammation, but shedding and dysregulation of bronchial epithelial repair contribute to airway hyper-reactivity in atopic asthmatics (29). Several studies have demonstrated that DEP elicit biological responses in bronchial epithelial cells (25–28). These effects include the release of proinflammatory mediators as well as the induction of mucoid hyperplasia (30–35). However, since these cells are not phagocytic and differ in many other respects from macrophages, the mechanism of PM action in epithelial cells is unknown. We do know that bronchial epithelial cells endocytose DEP and are able to mount biological responses to oxidative stress (33). However, the extent to which the oxidative stress response differs in epithelial cells and macrophages is unknown. This is a key area to explore, since rational therapy for the adverse health effects of PM should consider effective ways to curb the consequences of oxidative stress in the lung.

The aim of this study was to investigate the sensitivity of human bronchial epithelial cells to organic DEP chemicals and to determine whether there is a link between the level of oxidative stress and the cellular response. To perform these studies we compared normal human bronchial epithelial cells as well as a bronchial epithelial cell line, BEAS-2B, to macrophages. Our data demonstrate that while organic DEP extracts generate oxidative stress in epithelial cells, these cells differ from macrophages in the types of ROS being produced and the sensitivity to a programmed cell death pathway. Similar to THP-1 cells, there was good correlation between the extract dose, the drop in cellular GSH/GSSG ratios, and ensuing cellular responses. Unlike macrophages, *N*-acetylcysteine (NAC) was ineffective in protecting bronchial epithelial cells from cytotoxic death. These results suggest similarities as well as key differences between macrophages and epithelial cells in their responses to redox cycling DEP chemicals.

## Materials and Methods

### Reagents

RPMI 1640, DMEM, F12K Nutrient Mix (F12K), penicillin-streptomycin, and *L*-glutamine were obtained from Life Technologies (Gaithersburg, MD). Bronchial epithelial growth medium (BEGM) was purchased from Clonetics (Walkersville, MD). FBS was purchased from Irvine Scientific (Santa Ana, CA). Type I rat tail collagen was purchased from Collaborative Biotech (Bedford, MA). DEP were a gift from Dr. M. Sagai (National Institute of Environment Studies, Tsukuba, Japan). Anti-HO-1 mAb was purchased from Stressgen (Victoria, Canada). Anti-manganese superoxide dismutase (anti-MnSOD) Ab was obtained from Upstate Biotechnology (Lake Placid, NY). Monoclonal anti-phospho-JNK and polyclonal anti-JNK Abs were from Cell Signaling (Beverly, MA). Biotinylated rabbit anti-mouse and swine anti-rabbit Abs were obtained from Dako (Carpinteria, CA). HRP-conjugated sheep anti-mouse Ab was obtained from Amersham (Piscataway, NJ). Hydroethidine (HE), dihydrochlorofluorescein diacetate (DCF), 3,3'-dihydroxyoxycarbocyanine iodide (DiOC<sub>6</sub>), and the ATP assay kit were purchased from Molecular Probes (Eugene, OR). NAC, propidium iodide (PI), GSH, GSSG,  $\beta$ -NADPH, and glutathione reductase were obtained from Sigma (St. Louis, MO). Cobalt protoporphyrin (CoPP) was purchased from Porphyrin Products (Logan, UT). Annexin-FITC kit was purchased from Trevigen (Gaithersburg, MD). ECL reagents were purchased from Pierce (Rockford, IL).

### Cell culture

Human bronchial epithelial cells (BEAS-2B) and the human (THP-1) and murine (RAW 264.7) macrophage cell lines were obtained from American Type Culture Collection (Manassas, VA). Normal human bronchial epithelial cells (NHBE) were purchased from Clonetics (Walkersville, MD). Human pulmonary alveolar macrophages (PAM) were provided by Dr. J. Balmes (University of California, San Francisco, CA). THP-1 and PAM were cultured in RPMI 1640 supplemented with 10% FBS, penicillin/streptomycin, and glutamine. NHBE were cultured in BEGM. BEAS-2B cells were cultured in BEGM in type I rat tail collagen-coated flasks or plates.

RAW264.7 were grown in DMEM plus 10% FBS. All cell cultures were conducted in a 37°C humidified incubator supplied with 5% CO<sub>2</sub>.

### Preparation of DEP methanol extracts and cell stimulation

DEP methanol extracts were prepared as previously described (17). Briefly, 100 mg DEP were suspended in 25 ml methanol and sonicated for 2 min. The DEP methanol suspension was centrifuged at 2000 rpm for 10 min at 4°C. The methanol supernatant was transferred to a preweighed polypropylene tube and dried under nitrogen gas. The tube was reweighed to determine the amount of methanol-extractable DEP components. Dried DEP extract was then dissolved in DMSO at a concentration of 100  $\mu$ g/ $\mu$ l. The aliquots were stored at –80°C in the dark until use.

### Preparation of DEP fractions

Preparation of DEP fractions was conducted as previously described (11). Briefly, 1 g DEP was extracted with 60 ml methylene chloride five times using a VirTis homogenizer (Gardiner, NY). The combined extracts were concentrated by rotoevaporation, and asphaltene were precipitated by exchanging into hexane. The supernatant was concentrated, dried over anhydrous sodium sulfate, and subjected to silica gel column chromatography (column size, 1  $\times$  30 cm) following the method of Venkatesan et al. (11). Aliphatic, aromatic, and polar fractions were collected by elution with 20 ml hexane, 40 ml hexane/methylene chloride (3/2), and 30 ml methylene chloride/methanol (1/1), respectively. The fractions were weighed in a microbalance by evaporating off a known volume of an aliquot of the sample made up in methylene chloride or methanol. The fractions were dried with N<sub>2</sub> gas and redissolved in DMSO.

### Western blotting analysis

Western blotting was conducted as previously described (17). One hundred to 150  $\mu$ g total protein was separated by SDS-PAGE before transfer to polyvinylidene difluoride membranes. HO-1 protein was detected by anti-HO-1 mAb at 0.3  $\mu$ g/ml and rabbit anti-mouse Ab conjugated to HRP according to the manufacturer's instructions. Anti-MnSOD Ab was used at 0.3  $\mu$ g/ml. Biotinylated swine anti-rabbit Ab (1/1,000) was used as the secondary Ab, followed by HRP-conjugated avidin-biotin complex (1/10,000). Blots were developed with the ECL reagents according to the manufacturer's instruction. Phospho-JNK and JNK proteins were detected using monoclonal anti-phospho-JNK (1/1,000) and polyclonal anti-JNK (1:1,000) Abs. Biotinylated rabbit anti-mouse (1/1,000) and swine anti-rabbit (1/1,000) Abs were used as secondary Abs before HRP-conjugated avidin-biotin complex (1/10,000).

### RT-PCR analysis

Total RNA was extracted using TRIzol RNA extraction reagent (11). RT was performed at 42°C in a total volume of 20  $\mu$ l containing 5  $\mu$ g total RNA; 0.5  $\mu$ g oligo(dT)<sub>12–18</sub>; 10 mM DTT; 0.5 mM each of dATP, dGTP, dCTP, and dTTP; and 10 U Moloney murine leukemia virus reverse transcriptase (15). HO-1 primers for PCR amplification of a 350-bp human HO-1 fragment (36) were obtained from Life Technologies. The primer sequences of human HO-1 are 5'-CAGGCAGAGAATGCTGAGTT-3' and 5'-GCTTCACATAGCGCTGCA-3'. The sequences of human  $\beta$ -actin primers are 5'-TGAATCCTGTGGCATCCATGAAAC-3' and 5'-TAA AACGCAGCTCAGTAACAGTCCG-3'. PCRs for both HO-1 and  $\beta$ -actin were performed in a total reaction volume of 25  $\mu$ l containing 4  $\mu$ l cDNA template, 0.5  $\mu$ M sense and antisense primers, 1.5 mM MgCl<sub>2</sub>, 0.2 mM dNTP, and 2.5 U *Taq* DNA polymerase in a PerkinElmer thermal cycler (Norwalk, CT). Samples were heated to 95°C for 2 min and subjected to 35 cycles of amplification (30 s at 94°C, 60 s at 58°C, and 60 s at 72°C), followed by 7 min at 72°C for final extension. PCR products were electrophoresed in 2% agarose gels and viewed by ethidium bromide.

### Analysis of IL-8 production

After DEP stimulation, the culture media were collected and centrifuged to remove the debris. The media were frozen and sent to Cytokine Core Laboratories (Baltimore, MD) for measurement of the IL-8 levels by ELISA.

### Flow cytometry

ROS generation, mitochondrial membrane potential ( $\Delta\Psi$ m), and apoptosis were analyzed by flow cytometry using a FACScan equipped with an argon laser (BD Biosciences, Franklin Lakes, NJ) (17, 18). Superoxide radical (O<sub>2</sub><sup>•-</sup>) production and  $\Delta\Psi$ m were determined by dual staining with HE and DiOC<sub>6</sub>. Cells (10<sup>6</sup>/ml) were incubated with 2  $\mu$ M HE as well as 20 nM DiOC<sub>6</sub> diluted in the serum-free culture medium for 30 min in the dark at

37°C. Apoptosis was analyzed by annexin V-FITC/PI double staining according to the manufacturer's instructions. Time- and dose-dependent cellular cytotoxicity were determined by staining the cells in 1  $\mu\text{g}/\text{ml}$  PI. DiOC<sub>6</sub> and annexin V-FITC fluorescence were analyzed in the fluorescent-1 channel, while PI and HE fluorescence were analyzed in FL-2 and -3 channels, respectively.

#### Determination of GSH/GSSG ratio

Total glutathione (GSH plus 1/2 GSSG) and GSSG were measured in a recycling assay that uses 5,5'-dithio-bis(2-nitrobenzoic acid) and glutathione reductase (37–39). Briefly, cells were lysed and deproteinized in 3% 5-sulfosalicylic acid. Whole cell lysates were cleared by centrifugation at 4°C at 14,000 rpm in an Eppendorf centrifuge. The supernatant was used for the measurement of total and oxidized glutathione. The amount of total glutathione from each sample was calculated from a GSH standard curve prepared in 5-sulfosalicylic acid. For GSSG assay, 100  $\mu\text{l}$  supernatant was incubated with 2  $\mu\text{l}$  2-vinylpyridine and 6  $\mu\text{l}$  triethanolamine for 60 min on ice. GSSG standards were treated in the same way as samples. The amount of GSSG in the samples was calculated from the GSSG standard curve. The amount of reduced GSH was calculated by subtracting the amount of GSSG from that of total glutathione.

#### Electron microscopy

Procedures for routine electron microscopy have been previously described by Yang et al. in detail (40). Briefly, cells were fixed in glutaraldehyde and postfixed in osmium tetroxide. The cells were then dehydrated in a series of ethanol and embedded in Epon-Spurr. Thin sections for electron microscopy were cut with a Reichert-Jung Ultracut and Ultramicrotome (Vienna, Austria). Copper grids were stained with lead citrate and uranyl acetate and photographed in a Hitachi (Tokyo, Japan) electron microscope.

#### Measurement of cellular ATP levels

Cellular ATP levels were measured as previously described (12). Briefly, cells were harvested by scraping and were lysed in H<sub>2</sub>O. The cell lysates were boiled for 5 min, and the ATP concentration was determined using a luciferase assay kit according to the manufacturer's instruction.

#### Statistics

Data were analyzed using SAS statistical software (SAS Institute, Cary, NC). Scheffe's method of multiple comparisons with *F* test was used for ANOVA.

## Results

### Organic DEP extracts induce ROS production and oxidative stress effects in bronchial epithelial cells

Using macrophages as a target cell for DEP, we have previously demonstrated that these particles elicit biological effects that can be ascribed to their organic carbon content (7–9, 11–14, 20). Moreover, treatment of PAM or THP-1 cells with a methanol DEP extract mimics the effect of intact particles, including their ability to generate ROS. This effect can be demonstrated by DCF fluorescence, which reflects mostly H<sub>2</sub>O<sub>2</sub> production (17, 18). While treatment of the bronchial epithelial cell line BEAS-2B with the same type of extract failed to induce DCF fluorescence (data not shown), these cells demonstrated increased HE fluorescence (Fig. 1A). HE is oxidized to ethidium bromide by ROS and is mostly likely a reflection of O<sub>2</sub><sup>-</sup> production (18). In contrast to HE conversion in BEAS-2B cells, THP-1 cells did not exhibit an appreciable increase in HE fluorescence (Fig. 1A).

Cells use intracellular GSH to neutralize ROS and protect themselves against oxidative damage. In case of a vigorous antioxidant defense, intracellular GSH stores may become depleted, leading to a drop in GSH/GSSG ratios. When exposed to increasing amounts of a methanol DEP extract, both THP-1 and BEAS-2B cells exhibited a dose-dependent decrease (*p* < 0.005) in GSH/GSSG ratios (Fig. 1B). Similar changes in intracellular glutathione ratios

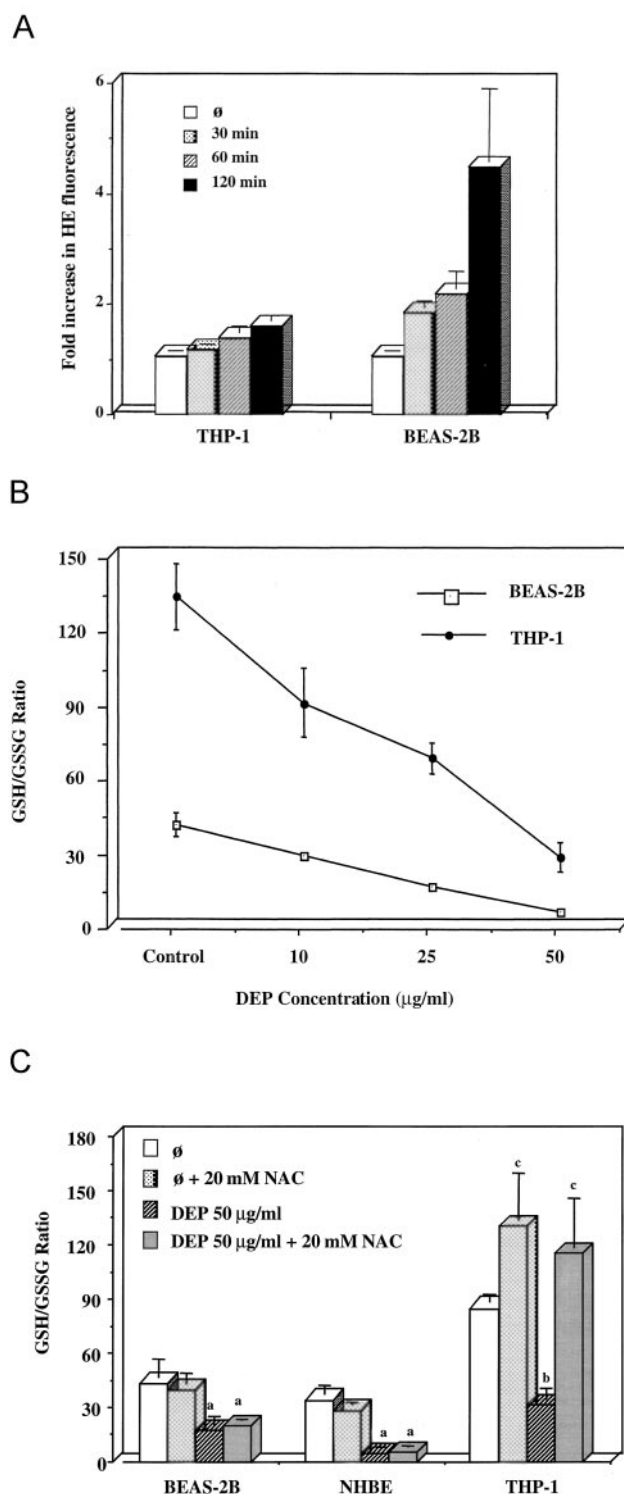


**FIGURE 1.** Alteration of cellular redox by an organic DEP extract and the effect of the antioxidant, NAC. *A*, Time-dependent increase in HE fluorescence. BEAS-2B and THP-1 cells were treated with 100  $\mu\text{g}/\text{ml}$  DEP extract for the indicated period. O<sub>2</sub><sup>-</sup> levels were analyzed by flow cytometry using HE staining as described in Materials and Methods. *B*, Dose-dependent decrease in the GSH/GSSG ratio induced by DEP extract. BEAS-2B and THP-1 cells were exposed to the indicated concentrations of DEP extract for 5 h. Determination of total and oxidized glutathione and GSH/GSSG ratios was performed as described in Materials and Methods. Values represent the mean  $\pm$  SEM. *p* < 0.005 at extract doses  $\geq$  10  $\mu\text{M}$ . *C*, The effects of NAC on cellular GSH/GSSG ratios. Cells were treated with 50  $\mu\text{g}/\text{ml}$  DEP extract for 5 h in the absence or the presence of 20 mM NAC. *a*, *p* < 0.005; *b*, *p* < 0.007 (compared with the controls). *c*, *p* = 0.0002 (compared with 50  $\mu\text{g}/\text{ml}$  DEP).

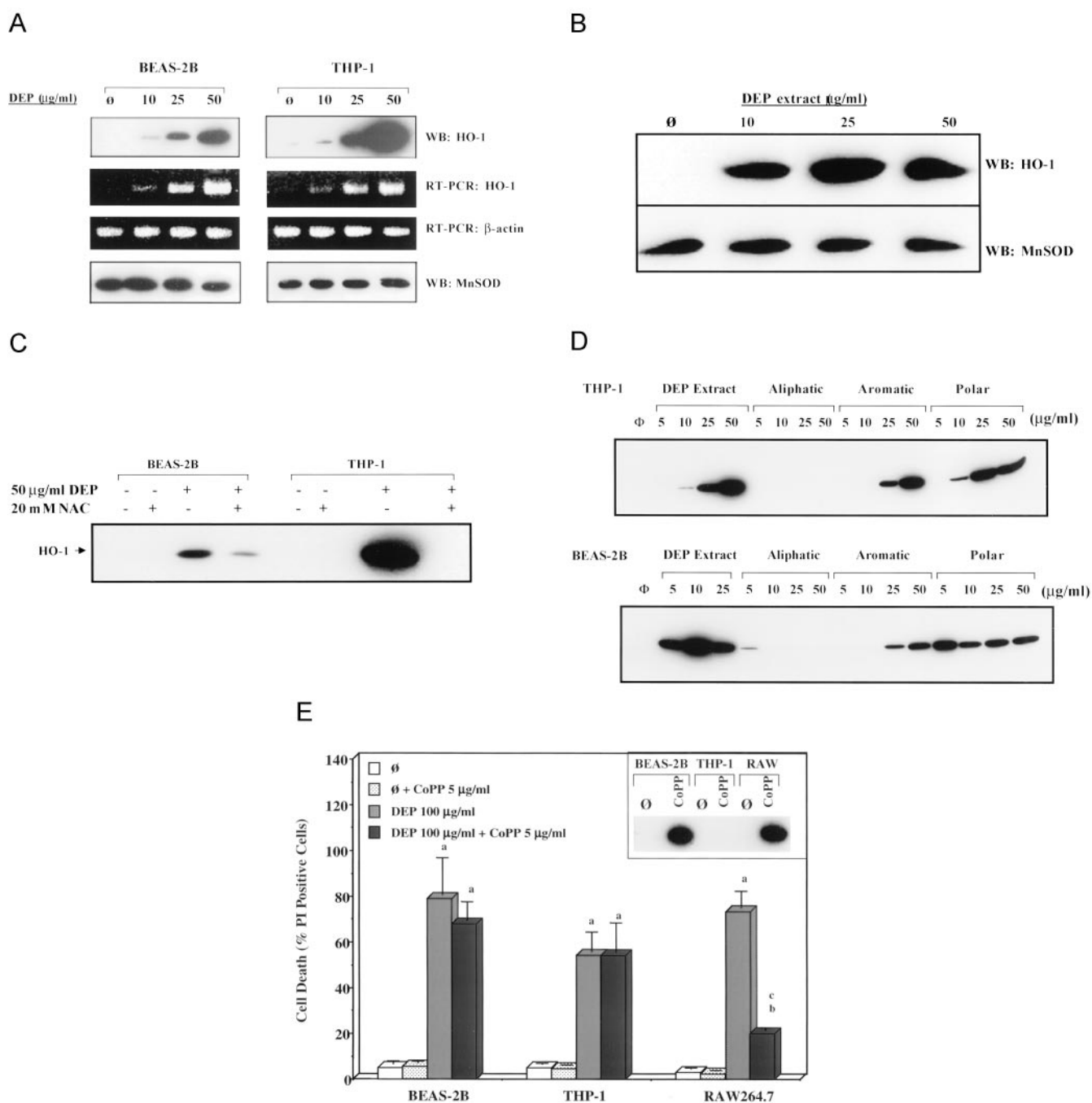


**FIGURE 2.** The effects of DEP extracts on cytoprotective pathways. *A*, Immunoblotting and RT-PCR demonstrating the effects of a DEP extract on HO-1 and MnSOD expression in BEAS-2B and THP-1 cells. Cells were stimulated with different concentrations of DEP extract as indicated for 5 h. Immunoblotting and RT-PCR were performed as described in *Materials and Methods*.  $\beta$ -Actin was used as an internal control. *B*, Western blotting showing the effects of DEP extract on HO-1 and MnSOD expression in NHBE cells. Cells were treated with the indicated concentrations of DEP extract for 5 h before being collected for SDS-PAGE and immunoblotting. *C*, The effect of NAC on HO-1 expression was demonstrated by immunoblotting. BEAS-2B and THP-1 cells were incubated with 20 mM NAC for 1 h before addition of 50  $\mu$ g/ml DEP extract for 5 h. *D*, The effects of aliphatic, aromatic, and polar chemical fractions on HO-1 expression. An organic DEP extract was fractionated by silica gel chromatography as previously described (15). The presence of alkenes, PAHs, and quinones in these respective fractions were confirmed by chemical analysis as previously described (15). The indicated amounts of the crude methanol extract as well as each fraction were incubated with THP-1 and BEAS-2B cells for 5 h before Western blotting. The small band in the aliphatic (5  $\mu$ g/ml) lane probably represents spillage from the 25  $\mu$ g/ml DEP sample. *E*, The effect of CoPP on DEP-induced cell death in BEAS-2B, THP-1, and RAW264.7 cells. Following preincubation with 5  $\mu$ g/ml CoPP for 48 h the cells were incubated with DEP extract (100  $\mu$ g/ml) in the continuous presence of CoPP for 16 h. Induction of HO-1 was determined by Western blotting (*inset*). Cell viability was analyzed by flow cytometry using PI staining. Values are the mean  $\pm$  SEM. a,  $p = 0.0001$ ; b,  $p = 0.0022$  (compared with the controls). c,  $p = 0.0001$  (compared with 100  $\mu$ g/ml DEP).

occurred in NHBE during exposure to the DEP extract (Fig. 1C). Interestingly, THP-1 cells maintain a higher basal GSH/GSSG ratio than BEAS-2B or NHBE cells (Fig. 1, B and C).

We have previously shown that thiol antioxidants are effective in preventing the oxidative stress effects of DEP chemicals (16). While NAC could increase basal GSH/GSSG ratios in THP-1

cells, this thiol antioxidant did not affect basal glutathione levels in BEAS-2B or NHBE cells (Fig. 1C). In addition, while NAC prevented a decline in GSH/GSSG ratios in THP-1 cells during exposure to a DEP extract, this agent did not prevent a drop in glutathione ratios in BEAS-2B and NHBE cells (Fig. 1C). This suggests that there is no NAC conversion to glutathione in epithelial cells.

A sustained drop in cellular GSH/GSSG ratios is indicative of a pro-oxidant state and leads to protective cellular responses. Examples include the inducible expression of MnSOD and HO-1 (24). While THP-1 and BEAS-2B cells showed constitutive MnSOD expression, the DEP extract induced HO-1 protein and mRNA expression in a dose-dependent fashion (Fig. 2A). In contrast, there was no change in the expression of a household gene,  $\beta$ -actin (Fig. 2A). Similarly, NHBE cells showed an increase in HO-1 expression, while MnSOD was constitutively expressed (Fig. 2B). The role of oxidative stress in HO-1 expression was confirmed by the ability of NAC to interfere with this response in BEAS-2B cells and macrophages (Fig. 2C). This suggests that although NAC is not converted to GSH in epithelial cells, this agent can function as a radical scavenger.

We have previously shown that the effect of the crude DEP extract on HO-1 expression can be mimicked by aromatic and polar chemical groups fractionated from these particles (11). We have also demonstrated that the aromatic fraction is enriched for PAHs, while the polar fraction includes quinones, but no PAHs (11). Using these materials, we showed dose-dependant HO-1 expression by polar and aromatic chemical groups in THP-1 cells (Fig. 2D). The polar was more potent than the aromatic fraction, while an aliphatic fraction lacked activity (Fig. 2D). The same trend was seen in BEAS-2B cells, except that the potency of the polar material was of sufficient magnitude to affect cell viability and HO-1 expression at doses  $>5 \mu\text{g/ml}$  (Fig. 2D). These results are in accordance with the ability of quinones to directly engage in redox cycling, while PAH require enzymatic conversion before being able to exert this effect (7).

We have previously demonstrated that CoPP-treated RAW264.7 cells are partially protected against the cytotoxic effects of redox cycling DEP chemicals (11) (Fig. 2E). CoPP is a non-heme HO-1 inducer (11). Interestingly, an attempt to induce HO-1 expression with CoPP in THP-1 cells failed, and these cells were not protected against DEP cytotoxicity (Fig. 2E). While CoPP was an effective HO-1 inducer in BEAS-2B cells, it did not protect those cells against the effect of oxidizing DEP chemicals (Fig. 2E). This suggests that despite its cytoprotective and antioxidant function, HO-1 is not sufficient to protect epithelial cells against the injurious effects of redox cycling DEP chemicals. The higher susceptibility of epithelial cells to cytotoxic DEP effects is discussed below.

Taken together, the above results demonstrate that organic DEP chemicals induce oxidative stress in bronchial epithelial cells. This leads to increased HO-1 expression, which commences at relatively low extract amounts ( $\leq 10 \mu\text{g/ml}$ ), and escalates as the level of oxidative stress increases. While this response mimics HO-1 expression in THP-1 cells, there is a difference in the kinetics and magnitude of  $\text{O}_2^-$  production in these cells as determined by HE fluorescence.

#### Organic DEP extracts induce JNK activation in bronchial epithelial cells

In addition to initiating antioxidant and cytoprotective responses, oxidative stress can activate intracellular signaling cascades, including the mitogen-activated protein kinase and NF- $\kappa$ B cascades. Treatment of THP-1 and BEAS-2B cells with an organic DEP extract led to JNK activation (Fig. 3A). Thus, increased phosphor-

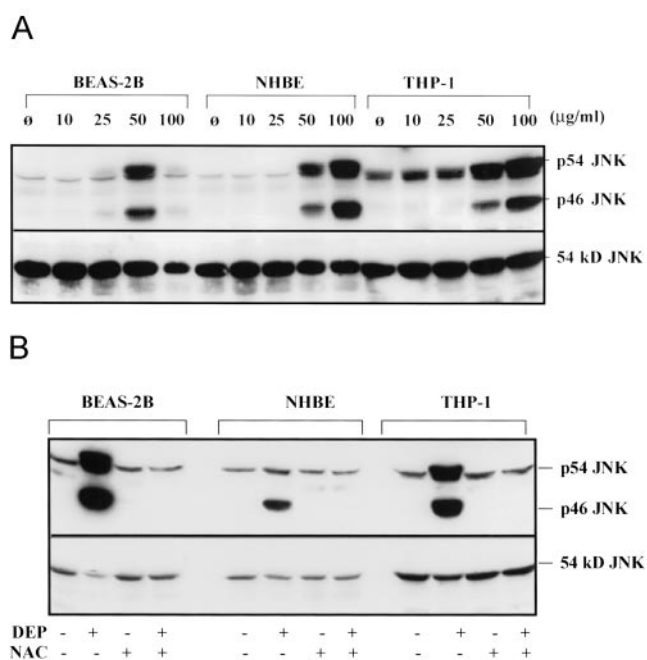


**FIGURE 3.** JNK activation by DEP extract and prevention by NAC. *A*, Dose-dependent activation of JNK by DEP extract. BEAS-2B, NHBE, and THP-1 cells were stimulated with the indicated concentrations of DEP extract for 2.5 h. Western blotting for phospho-JNK and JNK was conducted as described in *Material and Methods*. *B*, Inhibition of JNK activation by antioxidant, NAC. Cells were exposed to 50  $\mu\text{g/ml}$  DEP extract in the absence and the presence of 20 mM NAC. Immunoblotting was performed as described in *A*.

ylation of the 45- and 54-kDa JNK isoforms could be seen at extract doses  $\geq 25 \mu\text{g/ml}$ ; a high rate of cell death diminished the BEAS-2B response at 100  $\mu\text{g/ml}$  (Fig. 3A). NHBE also showed increased JNK phosphorylation in the dose range of 50–100  $\mu\text{g/ml}$  (Fig. 3A). These effects were not due to a decrease in the abundance of JNK protein, as demonstrated by anti-JNK immunoblotting (Fig. 3A, lower panel). The importance of oxidative stress in JNK activation was demonstrated by interference in p45 and p54 phosphorylation when assays were conducted in the presence of NAC (Fig. 3B). This again suggests that although not converted to glutathione, NAC functions as a radical scavenger in epithelial cells.

Taken together, the results in Fig. 3 demonstrate that at extract doses higher than that required to initiate HO-1 expression, organic DEP chemicals activate the JNK cascade in epithelial cells and macrophages. Since higher extract doses are associated with lower GSH/GSSG ratios (Fig. 1B), this suggests response stratification.

#### Organic DEP extracts induce IL-8 production in bronchial epithelial cells

A consequence of the activation of intracellular signaling cascades is the transcriptional activation of proinflammatory genes, including genes that encode for cytokines, chemokines, and adhesion receptors. One example is the IL-8 gene, which is under dual regulation by NF- $\kappa$ B and AP-1 response elements in its proximal promoter (41, 42). IL-8 is particularly relevant to the proinflammatory effects of DEP in the lung (22, 26–28). To compare IL-8 induction in epithelial and THP-1 cells, cultures were treated with 10–100  $\mu\text{g/ml}$  of the DEP extract for 14 h before measuring IL-8 in the culture medium. While THP-1 cells showed a dose-dependent response over the entire dose range (10–100  $\mu\text{g/ml}$ ), NHBE cells showed an incremental response in the range 10–50  $\mu\text{g/ml}$ ,

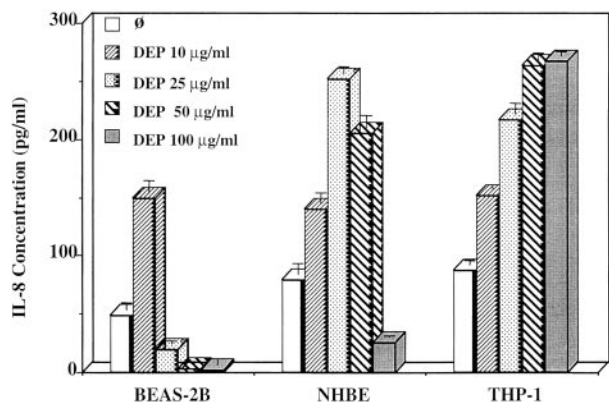


**FIGURE 4.** Increased IL-8 production by DEP extract. BEAS-2B, NHBE, and THP-1 cells were stimulated with the indicated concentrations of DEP extract for 14 h before culture media were collected. The IL-8 concentration in the medium was determined by ELISA as described in *Materials and Methods*. Values are the mean  $\pm$  SEM. Values of  $p = 0.0001$  compared with the controls. Note that for this time duration, there was a high rate of cell death in BEAS-2B cells at doses  $>10 \mu\text{g/ml}$  and in NHBE cells at doses  $>25 \mu\text{g/ml}$ .

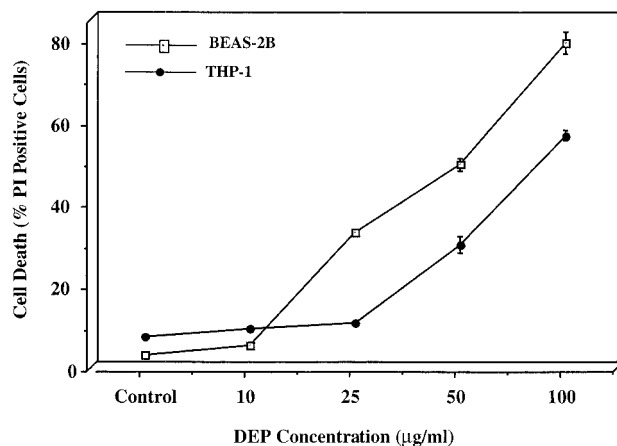
followed by a rapid decline at  $100 \mu\text{g/ml}$  (Fig. 4). This is probably due to a high rate of apoptosis in NHBE at doses  $>25 \mu\text{g/ml}$  (see below). While BEAS-2B responded to  $10 \mu\text{g/ml}$  of the extract, cellular toxicity led to a sharp drop in IL-8 production at higher doses (Fig. 4). These data strengthen the idea that incremental levels of oxidative stress lead to a transition from cytoprotective to injurious cellular responses.

#### *Organic DEP extracts induce cellular apoptosis and necrosis in epithelial cells by perturbation of mitochondrial function*

Previous studies from our laboratory demonstrated that intact DEP as well as organic extracts made from these particles induce a cytotoxic response in PAM and macrophage cell lines (17, 18). Compared with increased cytotoxicity at extract doses  $>25 \mu\text{g/ml}$  in THP-1 cells, BEAS-2B cells showed a significant rise in the rate of cell death at doses  $>10 \mu\text{g/ml}$  (Fig. 5A). Moreover, cell death commenced  $<2$  h in BEAS-2B cells, while increased PI uptake in THP-1 cells was delayed for at least 8 h or longer (Fig. 5B). NHBE cells also showed an enhanced rate of cytotoxicity compared with macrophages (not shown).

We have previously demonstrated that DEP cytotoxic effects in macrophages involve programmed cell death, dependent on the ability of these particles and their organic chemicals to generate oxidative stress (17, 18). This death event is characterized by the appearance of apoptotic bodies in epithelial cells and macrophages as well as positive annexin V/PI staining during two-color flow cytometry (Table I and Fig. 6). The annexin V<sup>+</sup>/PI<sup>+</sup> population was especially prominent in the BEAS-2B and NHBE populations, while THP-1 and PAM stained mostly PI positively, but annexin V negatively (Table I). While the exact reason for this difference in membrane asymmetry is unclear, it is possible that macrophages more rapidly degrade annexin V on the cell surface. We have previously shown that the percentage of annexin V<sup>+</sup>/PI<sup>+</sup> macrophages is more prominent at DEP extract doses  $<100 \mu\text{g/ml}$  (18). Treatment of human PAM and THP-1 cells with NAC interfered significantly in the generation of cytotoxicity (Table I). In contrast, NAC did not appreciably decrease the number of dead cells in the BEAS-2B and NHBE populations (Table I). Although this may suggest that epithelial toxicity is not dependent on oxidative stress, it should be noted that NAC is ineffective in preventing glutathione

**A**



**B**

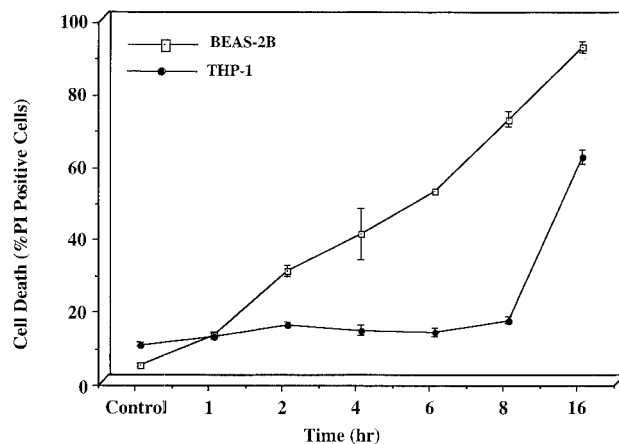


**FIGURE 5.** Cytotoxic effects of DEP extract on BEAS-2B and THP-1. The percentage of dead cells was determined by flow cytometry, using PI staining. Values represent the mean  $\pm$  SEM. *A*, Dose-dependent increases in cell death. Cells were treated with different concentrations of DEP extract for 16 h. *B*, Time course of DEP toxicity. BEAS-2B and THP-1 cells were exposed to  $100 \mu\text{g/ml}$  DEP extract for the indicated time before staining for flow cytometry.

depletion in epithelial cells (Fig. 1C). There is good evidence linking GSH depletion to the induction of apoptosis via a mitochondrial effect (17, 18, 43). Indeed, ultramicroscopic visualization of THP-1 and BEAS-2B cells showed that the appearance of apoptotic bodies is accompanied by changes in the mitochondrial morphology (Fig. 6, A and B). These changes, which include mitochondrial swelling as well as a loss of cristae, are indicative of apoptosis-necrosis and may represent a change in mitochondrial function (Fig. 6). Similar changes were seen in NHBE cells (not shown).

To study changes in mitochondrial function, we used dual-color DiOC<sub>6</sub> and HE fluorescence (Fig. 7). The resulting flow diagram shows that the DEP extract induced a decrease in the mitochondrial membrane potential (DiOC<sub>6</sub> fluorescence, lower left (LL) and upper left (UL) quadrants) as well as an increase in O<sub>2</sub><sup>-</sup> generation (HE fluorescence, UL and upper right (UR) quadrants) in BEAS-2B and THP-1 cells (Fig. 7). More specifically, the number of HE<sup>bright</sup> cells (UR quadrant) in the BEAS-2B population increased from 1.4 to 74.9% within 2 h of introducing the DEP extract (Fig. 7A). At this point, there was no drop in  $\Delta\Psi_m$ , but the

Table I. The effects of NAC (20 mM) on DEP-induced apoptosis in BEAS-2B, NHBE, PAM, and THP-1<sup>a</sup>

Cell Type Treatment	% of Cells			
	Annexin <sup>-</sup> /PI <sup>-</sup>	Annexin <sup>+</sup> /PI <sup>-</sup>	Annexin <sup>+</sup> /PI <sup>+</sup>	Annexin <sup>-</sup> /PI <sup>+</sup>
THP-1				
Φ	89.0	3.0	3.8	4.2
Φ + NAC	87.8	4.8	4.3	3.1
DEP 100 μg/ml	12.8	0.2	9.5	77.5
DEP + NAC	50.1	3.9	9.4	36.7
PAM				
Φ	89.2	3.9	4.1	2.8
Φ + NAC	86.9	0.6	2.7	9.8
DEP 100 μg/ml	6.7	0	0.02	93.3
DEP + NAC	76.4	2.4	11.5	9.8
BEAS-2B				
Φ	93.0	0.3	1.5	5.3
Φ + NAC	89.9	1.2	3.5	5.4
DEP 100 μg/ml	0.9	0.03	65.1	34.1
DEP + NAC	5.4	0.02	52.2	42.4
NHBE				
Φ	90.8	0.1	0.8	8.3
Φ + NAC	88.3	0.1	0.9	10.6
DEP 100 μg/ml	5.8	0	35.9	58.3
DEP + NAC	1.3	0.3	43.2	55.2

<sup>a</sup> Cells were treated with DEP extract (100 μg/g/ml) with or without 20 mM NAC for 16 h. Apoptosis was determined by flow cytometry using annexin V and PI double staining as described in *Materials and Methods*.

number of DiOC<sub>6</sub><sup>low</sup> cells increased to 40.2% (LL and UL quadrants) by 7 h (Fig. 7A). Although the extract-induced increase in HE fluorescence was not as pronounced in NHBE, the drop in the ΔΨ<sub>m</sub> was more pronounced than that in BEAS-2B cells (Fig. 7B, LL and UL quadrants). In contrast to epithelial cells, the number of THP-1 cells showing an increase in O<sub>2</sub><sup>-</sup> production after 2 and 7 h was limited to 20 and 10% (UR quadrant), respectively (Fig. 7A). These results agree with the data in Fig. 1A, which show higher HE fluorescence in BEAS-2B compared with THP-1 cells. Moreover, the drop in ΔΨ<sub>m</sub> cells was limited to <20% (LL and UL quadrants) in THP-1 cells (Fig. 7A).

Apoptosis-necrosis is a process in which the morphological features of apoptosis (e.g., the presence of apoptotic bodies) is combined with the features of cellular necrosis (mitochondrial disintegration and cellular fractionation). A key feature of apoptosis-necrosis is the inability to sustain ATP production due to damage to the mitochondrial inner membrane. Direct measurement of cellular ATP levels demonstrated a sharp and precipitous ( $p = 0.0001$ ) drop in ATP levels in BEAS-2B cells (Fig. 8). Similarly, ATP levels in NHBE cells decreased by >80% within 2 h of stimulation ( $p = 0.0001$ ) and remained low thereafter (Fig. 8). In contrast, the rate of ATP decline in THP-1 cells was slower and only reached the epithelial low point by 8 h (Fig. 8). The significance of apoptosis-necrosis is that residual cellular fragments are proinflammatory, while apoptotic bodies are removed in a "silent" manner.

Taken together, the data in Figs. 4–8 indicate that at relatively high concentrations of DEP extract, there is a transition from cytoprotective to cytotoxic effects. This idea is compatible with a stratified oxidative stress model in which antioxidant responses transition to proinflammatory and cytotoxic effects as the level of oxidative stress increases.

## Discussion

We demonstrate that organic DEP extracts, including polar and aromatic fractions, induce oxidative stress in epithelial cells, in response to which these cells exhibit HO-1 expression, JNK activation, IL-8 production and induction of apoptosis-necrosis. While

THP-1 cells responded in similar fashion, epithelial cells produced more O<sub>2</sub><sup>-</sup> and were more susceptible to cytotoxic effects than macrophages. Cytotoxicity is the result of mitochondrial damage, which manifests as a decrease in the ΔΨ<sub>m</sub>, ROS production, and ATP depletion. Another key difference between epithelial cells and macrophages is the ability of NAC to elevate GSH/GSSG ratios and prevent cytotoxicity in macrophages, while failing to do so in epithelial cells. Since treatment with NAC interfered with JNK activation and HO-1 expression in epithelial cells, this suggests that despite acting as a radical scavenger, this thiol agent is not converted to glutathione in epithelial cells. Induction of HO-1 expression at a low extract dose coincides with a minimal change in the GSH/GSSG ratio, while IL-8 production and JNK activity commences at 10–50 μg/ml, a dose leading to a more drastic decline in GSH/GSSG levels. While induction of cellular toxicity in THP-1 cells required an extract dose >25 μg/ml, the onset of cell death in BEAS-2B cells was more linear at doses ≥10 μg/ml.

The data in this study are of considerable importance to the priorities for airborne particulate matter as formulated by an expert committee of the National Academy of Sciences (6). Among the committee's top 10 priorities, particular emphasis is given to the elucidation of molecular mechanisms by which ambient airborne PM cause adverse health effects (6). We are particularly interested in the role of organic chemical compounds and have selected DEP as a model air pollutant to clarify some of these mechanistic issues (8). The idea that PAH and their oxygenated derivatives on DEP (e.g., quinones) participate in redox cycling and ROS generation was confirmed by the data in Fig. 2D showing that aromatic and polar compounds fractionated from DEP by silica gel chromatography induce HO-1 expression (11). These fractions are enriched for PAH and quinones, respectively. It is important to clarify that our data do not exclude the contribution of transition metals and other PM components in the biological effects of PM.

GSH and GSSG are the major redox pair involved in cellular redox homeostasis. A decline in the cellular GSH/GSSG ratio is regarded as a representative marker for oxidative stress and is directly responsible for the perturbation of cellular function (7, 44–



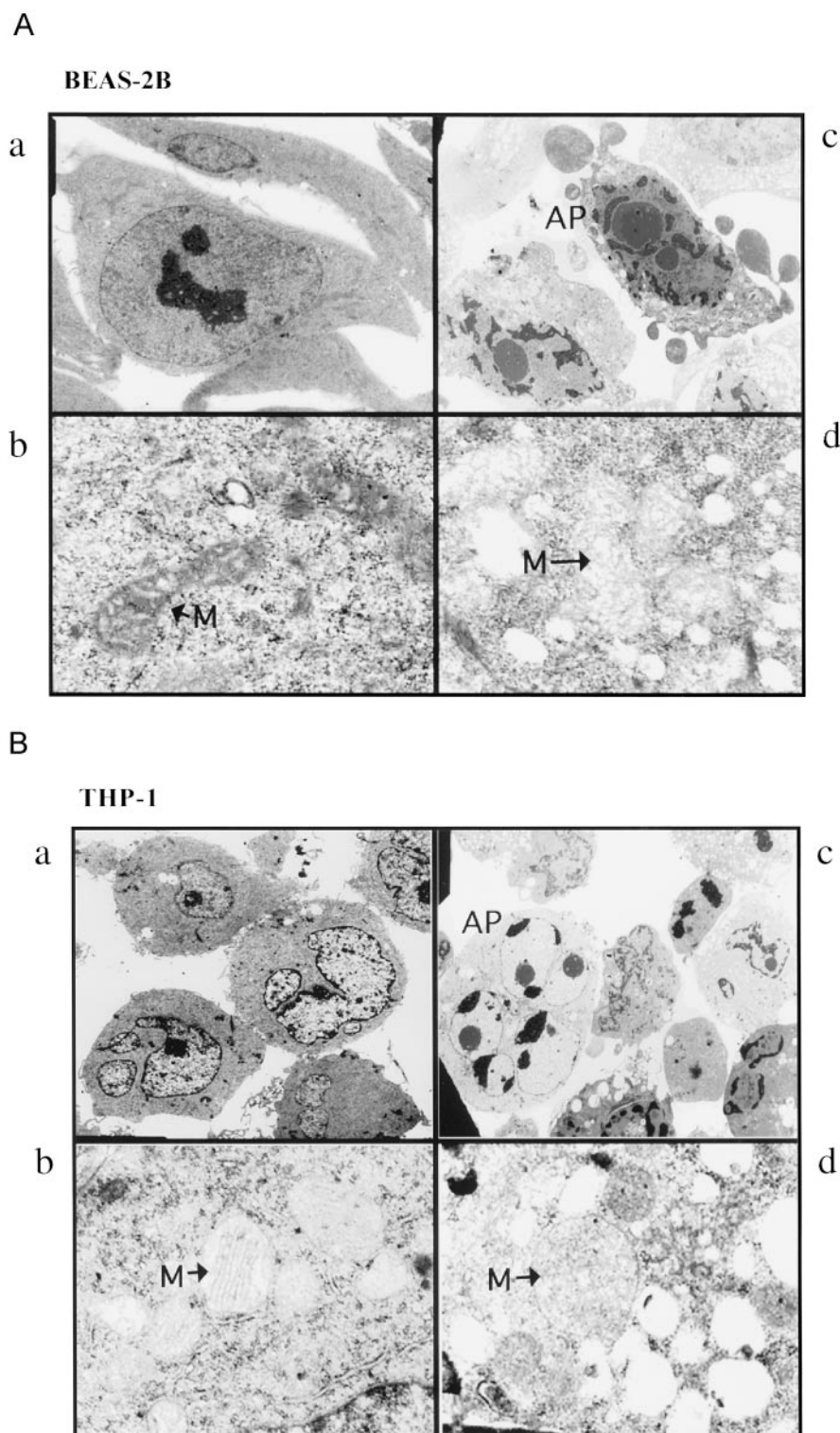


**FIGURE 6.** Electron microscopy showing structural features of cell death. Cells were treated with 100  $\mu\text{g/ml}$  DEP extract for 6 h before being fixed for electron microscopic study. Electron microscopy was performed as described in *Materials and Methods*. *A*, BEAS-2B. *a* and *b*, Control; *c* and *d*, DEP-treated cells. Magnification: *a*,  $\times 3500$ ; *b*,  $\times 15,100$ ; *c*,  $\times 2400$ ; *d*,  $\times 12,400$ . *B*, THP-1. Magnification: *a*,  $\times 2800$ ; *b*,  $\times 15,100$ ; *c*,  $\times 2,400$ ; *d*,  $\times 15,100$ . AP, apoptotic body; M, mitochondrion.

46). This includes activation of antioxidant defense pathways, as well as induction of proinflammatory and cytotoxic responses (24). An interesting difference between epithelial cells and macrophages is the lower basal GSH/GSSG ratios in the former compared with the latter cell type (Fig. 1). This may explain the increased propensity toward cytotoxicity in epithelial cells.

An example of a cellular antioxidant defense mechanism is HO-1 expression (11, 47). Not only does HO-1 constitute a very sensitive marker of oxidative stress, but its catalytic action on heme generates a potent antioxidant, bilirubin, as well as a gaseous substance, CO, that exert anti-inflammatory effects in the lung (48). Not surprising, therefore, the CO level in exhaled air is a

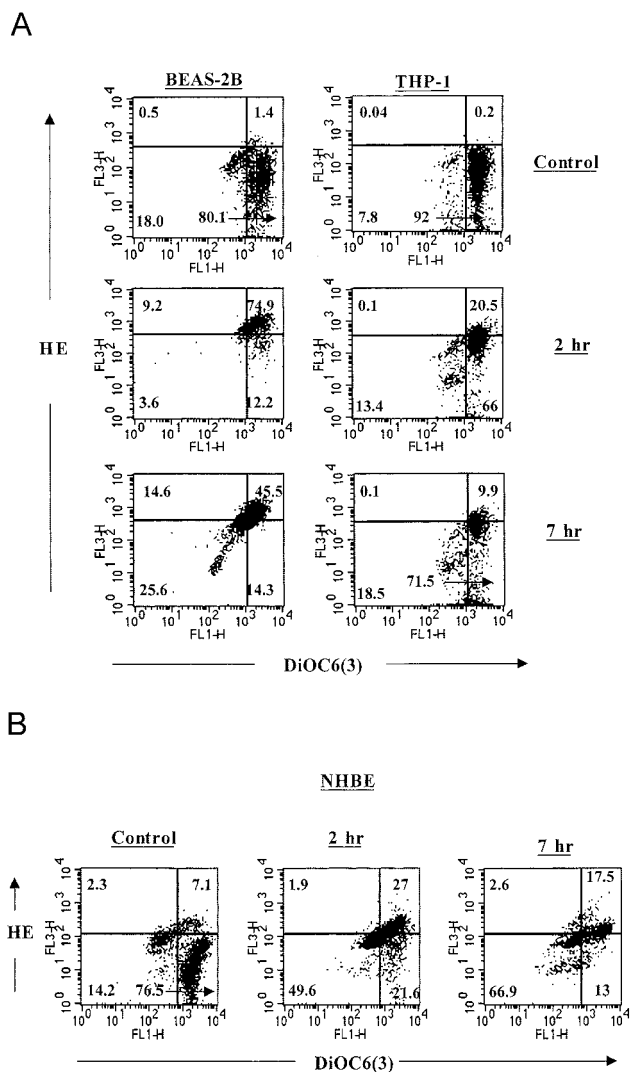


**FIGURE 7.** Mitochondrial functional perturbation.  $O_2^-$  and mitochondrial  $\Delta\Psi$  were measured by flow cytometry using dual-color HE/DiOC<sub>6</sub> staining as described in Materials and Methods. Definitions of quadrants: LL, DiOC<sub>6</sub><sup>low</sup>/HE<sup>low</sup>; UL, DiOC<sub>6</sub><sup>low</sup>/HE<sup>bright</sup>; lower right (LR), DiOC<sub>6</sub><sup>bright</sup>/HE<sup>low</sup>; and upper right (UR), DiOC<sub>6</sub><sup>bright</sup>/HE<sup>bright</sup>. A, DEP-induced changes in  $O_2^-$  and mitochondrial  $\Delta\Psi$  in BEAS-2B and THP-1. Cells were exposed to 100  $\mu$ g/ml DEP extract for 2 or 7 h. B, Dual-color analysis in NHBE cells. Cells were treated with 100  $\mu$ g/ml DEP extract for 2 or 7 h before staining for flow cytometry.

sensitive *in vivo* marker for the proinflammatory effects of DEP in the lung (49). The molecular basis for initiating this antioxidant defense mechanism is the transcriptional activation of the HO-1 gene by a series of ARE in its promoter (11, 47). It has now been established that the transcription factor Nrf-2 is involved in ARE activation *in vivo* and *in vitro* (50, 51). Not only have we confirmed that ARE is involved in activation of the HO-1 promoter by aromatic and polar DEP chemicals in macrophages (11), but we also demonstrate exquisite sensitivity of HO-1 to oxidative stress in epithelial cells (Fig. 2, A and B). However, while HO-1 exerts a cytoprotective effect in RAW264.7 cells, it failed to do so in BEAS-2B cells despite the fact that HO-1 expression could be induced by CoPP (Fig. 2B). This susceptibility may be due to the lower basal GSH/GSSG ratios in bronchial epithelial cells (Fig. 1B).

If of sufficient intensity, oxidative stress can initiate proinflammatory effects in macrophages and bronchial epithelial cells (21–23, 27, 32). These effects are mediated by phosphorylation-dependent cell

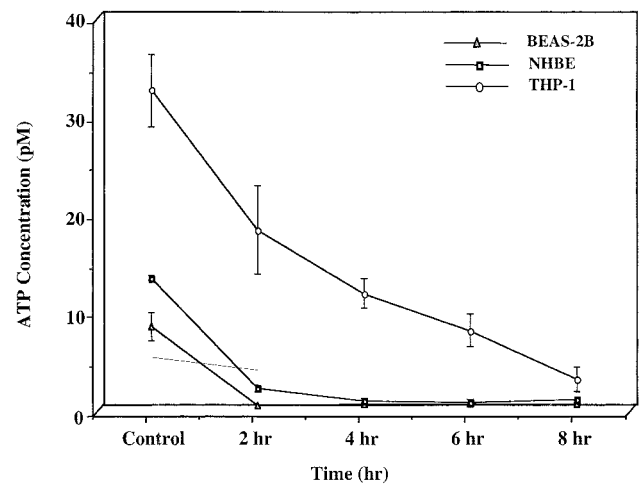


**FIGURE 8.** Kinetics of DEP-induced decline in ATP levels. Cells were treated with DEP extract (100  $\mu$ g/ml) for the indicated time period. The ATP concentration was determined by luciferase assay following the manufacturer's instructions. Values are the mean  $\pm$  SEM. For BEAS-2B,  $p < 0.0009$ ; for THP-1,  $p < 0.0001$ .

signaling pathways, including activation of the mitogen-activated protein kinase and NF- $\kappa$ B kinase cascades. In this communication we demonstrate that organic DEP extracts activate the JNK cascade in BEAS-2B and NHBE cells in a dose-dependent fashion (Fig. 3B). Interestingly, JNK activation required higher extract doses than that needed to initiate HO-1 expression, suggesting that this may constitute a hierarchical oxidative stress effect (Figs. 2A and 3A). This idea is in agreement with the progressive decrease in GSH/GSSG ratios at higher extract doses (Fig. 1B). The importance of JNK activation is that this may lead to transcriptional activation of proinflammatory cytokines and chemokines (8, 28, 52, 53). An example is IL-8 production, which could be induced by DEP extracts in BEAS-2B and NHBE cells (Fig. 4). While this response achieved a plateau at 25–50  $\mu$ g/ml in NHBE, there was a precipitous decline in IL-8 production in BEAS-2B at doses  $> 10$   $\mu$ g/ml. This is probably due to the higher rate of apoptosis in BEAS-2B cells.

Another consequence of oxidative stress is the induction of cellular apoptosis and necrosis (Fig. 5, A and B, and Table I). In this regard we have demonstrated that organic DEP chemicals induce cellular apoptosis and necrosis through perturbation of the mitochondrial PT pore (17, 18). A variety of redox cycling and oxidizing chemicals has been shown to perturb the PT pore (18, 54, 55). This leads to a cascade of events that includes a decrease in  $\Delta\Psi_m$ , cytochrome *c* release, and activation of cellular caspases (Fig. 7, A and B, and Table I). Damage to the mitochondrial inner membrane also disrupts four-electron reductions of  $O_2$ , switching this process instead to one-electron reductions (56, 57). This leads to  $O_2^-$  generation and could be responsible for the increased HE fluorescence shown in Fig. 7. Ultimately, damage to the inner membrane and interference in electron transfers lead to decreased ATP production and energy failure (Fig. 8). This leads to cellular necrosis, reflected by mitochondrial swelling and appearance of PI<sup>+</sup>/annexin V<sup>-</sup> cells, in addition to other features of apoptosis (Fig. 6).

Epithelial cells appear to be more susceptible to the cytotoxic effects of DEP extracts than macrophages (Table I and Fig. 5, A and B). While the reason for this increased susceptibility is unknown, we know that cellular GSH levels play a role in regulating mitochondrial permeability transition, possibly by preventing the

cross-linking of vicinal thiol groups in the PT pore (58). Although GSH predominates in the cytoplasm, a small portion is sequestered in mitochondria (59). Moreover, it has been suggested that GSH is the only antioxidant that protects mitochondria against the harmful effects of  $H_2O_2$  (59). Lower GSH/GSSG ratios in bronchial epithelial cells may limit their ability to protect the mitochondrial PT pore and may render these cells more susceptible to DEP-induced oxidative stress. The same reasoning may apply to the failure of NAC to protect bronchial epithelial cells (Table I). While this antioxidant effectively prevents decline of the GSH/GSSG ratios in THP-1 cells, NAC did not exert the same effect in bronchial epithelial cells (Fig. 1C). A possible explanation for this finding is that the drug is not deacetylated to the glutathione precursor in epithelial cells. The fact that NAC can prevent JNK activation and HO-1 expression in epithelial cells (Figs. 2C and 3B) may be related to its activity as a radical scavenger. Taking all these data into consideration, NAC may be a valuable therapeutic agent that can be used to modify macrophage and epithelial activation, as demonstrated by its ability to modulate biomarker induction by air particulate matter in rat and murine lung (16, 60). NAC also interferes in TNF- $\alpha$  production in alveolar macrophages exposed to air PM (61).

The above studies indicate that organic DEP extracts that are enriched for PAH and oxy-PAHs induce a range of biological effects related to the generation of oxidative stress. We propose that this constitutes a stratified cellular response to oxidative stress. At the lower end of the oxidative stress scale, cells or tissues are stimulated to induce ARE-dependent antioxidant and cytoprotective responses. If these protective mechanisms fail, further escalation of oxidative stress may lead to proinflammatory or cytotoxic effects. We propose that activation of intracellular signaling cascades, e.g., the JNK pathway, and perturbation of the mitochondrial PT pore play a role in these injurious cellular responses. This implies that the activation threshold for cellular injury requires higher oxidative stress levels than those required for cytoprotective responses.

A stratified oxidative stress model may prove useful in study of the adverse health effects of PM. Although some adverse effects may occur independently of oxidative stress, a stratified stress model implies that biological end points should be selected relevant to the level of oxidative stress and PM exposure. For instance, under the experimental conditions chosen by Nightingale et al. (49), an increased CO level in the expired air was a more sensitive end point than the bronchoalveolar neutrophil content. This agrees with the idea that HO-1 is a more sensitive oxidative stress marker than IL-8 (Fig. 2, A and B). Other ARE-driven events, e.g., expression of phase II drug-metabolizing enzymes (62), may be induced at this low stress level. When exposed to higher PM chemical doses, screening should include markers for inflammation, including cytokines and chemokines. This approach has been demonstrated in DEP nasal challenge studies in atopic individuals (9). Finally, it is important to consider that high levels of oxidative stress may induce cytotoxic effects, which could override and conceal the proinflammatory effects of the PM. One possibility is that apoptosis of macrophages and participating immune cells may interfere with allergic inflammation, but could still exacerbate asthma due to bronchial epithelial shedding.

Another value of the oxidative stress theory is that it may assist in the identification of human subsets that are more susceptible to the adverse health effects of PM. An example is HO-1 expression. This enzyme has potent antioxidant and cytoprotective effects in the lung (63). Noteworthy, a polymorphism of the HO-1 promoter has been described that reflects gene expression in the presence of ROS (64). Moreover, it has been demonstrated that male smokers

with a poorly responsive HO-1 promoter have a higher rate of emphysema than male smokers with a more inducible HO-1 gene (64). The same paradigm may apply to antioxidant and detoxification pathways that play a role in defending against the adverse biological effects of PM.

In conclusion, we have shown that organic DEP chemicals induce a range of biological responses in epithelial cells and macrophages that depend on the generation of oxidative stress. Epithelial cells appear to be more sensitive than macrophages, possibly due to a limited ability to defend them against oxidative stress. This is true even in the presence of a thiol antioxidant.

## References

- Pope, C. A., M. J. Thun, M. M. Nambodiri, D. W. Dockery, J. S. Evans, F. E. Speizer, and C. W. Heath, Jr. 1995. Particulate air pollution as a predictor of mortality in a prospective study of U.S. adults. *Am. J. Respir. Crit. Care Med.* 151:669.
- Dockery, D. W., C. A. Pope, X. Xu, J. D. Spengler, J. H. Ware, M. E. Fay, B. G. Ferris, and F. E. Speizer. 1993. An association between air pollution and mortality in six U.S. cities. *N. Engl. J. Med.* 29:1753.
- Pope, C. A., and D. W. Dockery. 1998. Epidemiology of particle effects. In *Air Pollution and Health*. S. T. Holgate, J. M. Samet, H. S. Koren, and R. L. Maynard, eds. Academic Press, London, p. 673.
- Pope, C. A. 1999. Mortality and air pollution: associations persist with continued advances in research methodology. *Environ. Health Perspect.* 107:613.
- Pope, C. A., D. W. Dockery, R. E. Kanner, G. M. Villegas, and J. Schwartz. 1999. Oxygen saturation, pulse rate, and particulate air pollution: a daily time-series panel study. *Am. J. Respir. Crit. Care Med.* 159:365.
- National Research Council. 1998. Research Priorities for Airborne Particulate Matter. I. Immediate Priorities and a Long-Range Research Portfolio. National Academy of Science, Washington, D.C.
- Nel, A. E., D. Diaz-Sanchez, and N. Li. 2001. The role of particulate pollutants in pulmonary inflammation and asthma: evidence for the involvement of organic chemicals and oxidative stress. *Curr. Opin. Pulmonary Med.* 7:20.
- Nel, A. E., D. Diaz-Sanchez, D. Ng, T. Hiura, and A. Saxon. 1998. Enhancement of allergic inflammation by the interaction between diesel exhaust particles and the immune system. *J. Allergy Clin. Immunol.* 102:539.
- Diaz-Sanchez, D., M. Jyrala, D. Ng, A. Nel, and A. Saxon. 2000. In vivo nasal challenge with diesel exhaust particles enhances expression of the CC chemokines RANTES, MIP-1 $\alpha$ , and MCP-3 in humans. *Clin. Immunol.* 97:140.
- Sagai, M., H. Saito, T. Ichinose, M. Kodama, and Y. Morri. 1993. Biological effects of diesel exhaust particles. In vitro production of superoxide and in vivo toxicity in mouse. *Free Radical Biol. Med.* 14:37.
- Li, N., M. I. Venkatesan, A. Miguel, R. Kaplan, C. Gujuluva, J. Alam, and A. E. Nel. 2000. Induction of heme oxygenase-1 expression in macrophages by diesel exhaust particle chemicals and quinones via the antioxidant-responsive element. *J. Immunol.* 165:3393.
- Schuetzle, D., F. S. Lee, and J. J. Prater. 1981. The identification of polynuclear aromatic hydrocarbon (PAH) derivatives in mutagenic fractions of diesel particulate extracts. *Int. J. Environ. Anal. Chem.* 9:93.
- Anderson, H., E. Lindqvist, R. Westerholm, K. Gragg, J. Almen, and L. Olson. 1998. Neurotoxic effects of fractionated diesel exhaust following microinjections in rat hippocampus and striatum. *Environ. Res.* 76:41.
- Li, H., C. D. Banner, G. G. Mason, R. N. Westerholm, and J. J. Raftar. 1996. Determination of polycyclic aromatic compounds and dioxin receptor ligands present in diesel exhaust particulate extracts. *Atmos. Environ.* 30:3537.
- Kumagai, Y., T. Arimoto, M. Shinyashiki, N. Shimojo, Y. Nakai, T. Yoshikawa, and M. Sagai. 1997. Generation of reactive oxygen species during interaction of diesel exhaust particle compounds with NADPH-cytochrome P450 reductase and involvement of the bioactivation in the DNA damage. *Free Radical Biol. Med.* 22:479.
- Whitekus, M. J., N. Li, M. Zhang, M. Wang, M. A. Horwitz, S. K. Nelson, L. D. Horwitz, N. Brechun, D. Diaz-Sanchez, and A. Nel. 2002. Thiol antioxidant inhibit the adjuvant effects of aerosolized diesel exhaust particles in a murine model for ovalbumin sensitization. *J. Immunol.* 168:2560.
- Hiura, T. S., M. P. Kaszubowski, N. Li, and A. E. Nel. 1999. Chemicals in diesel exhaust particles generate reactive oxygen radicals and apoptosis in macrophages. *J. Immunol.* 163:5582.
- Hiura, T. S., N. Li, R. Kaplan, M. Horwitz, J. Seagrave, and A. E. Nel. 2000. The role of a mitochondrial pathway in the induction of apoptosis by chemicals extracted from diesel exhaust particles. *J. Immunol.* 165:2703.
- Squadrio, G. L., R. Cueto, B. Dellinger, and W. A. Pryor. 2001. Quinoid redox cycling as a mechanism for sustained free radical generation by inhaled airborne particulate matter. *Free Radical Biol. Med.* 31:1132.
- MacNee, W., and K. Donaldson. 1998. Particulate air pollution: injurious and protective mechanisms in the lung. In *Air Pollution and Health*, Vol. 30. S. T. Holgate, J. M. Samet, H. S. Koren, and R. L. Maynard, eds. Academic Press, London, pp. 653–672.
- Alsberg, T., U. Stenberg, R. Westerholm, M. Strandell, U. Rannug, A. Sundvall, L. Romert, U. Bernson, B. Perterson, R. Toftgard, et al. 1985. Chemical and biological characterization of organic material from gasoline exhaust particles. *Environ. Sci. Technol.* 19:43.

22. Becker, S., J. M. Soukup, M. I. Gilmour, and R. B. Devlin. 1996. Stimulation of human and rat alveolar macrophages by urban air particulates: effects on oxidant radical generation and cytokine production. *Toxicol. Appl. Pharmacol.* 141:637.
23. Goldsmith, C., C. Frevort, A. Imrich, C. Sioutas, and L. Kobzik. 1997. Alveolar macrophage interaction with air pollution particulates. *Environ. Health Perspect.* 105:1191.
24. Li, N., S. Kim, M. Wang, J. Froines, C. Sioutas, and A. E. Nel. 2001. Evidence for the use of a stratified oxidative stress model to study the biological effects of ambient concentrated and diesel exhaust particulate matter. *Inhalation Toxicol.* 14:101.
25. Martin, L. D., T. M. Krunkovskiy, J. A. Dye, B. M. Fischer, N. F. Jiang, L. G. Rochelle, N. J. Akley, K. L. Dreher, and K. B. Adler. 1997. The role of reactive oxygen and nitrogen species in the response of airway epithelium to particulates. *J. Environ. Health Perspect.* 105:1301.
26. Bayram, H., J. L. Devalia, O. A. Khair, M. Muntasir, M. B. Abdelazia, R. J. Sapsford, M. Sagai, and R. J. Davies. 1998. Comparison of ciliary activity and inflammatory mediator release from bronchial epithelial cells of nonatopic nonasthmatic subjects and atopic asthmatic patients: the effects of diesel exhaust particles in vitro. *J. Allergy Clin. Immunol.* 102:771.
27. Ohtoshi, T., H. Takizawa, H. Okazaki, S. Kawasaki, N. Takeuchi, K. Ohta, and K. Ito. 1998. Diesel exhaust particles stimulate human airway epithelial cells to produce cytokines relevant to airway inflammation in vitro. *J. Allergy Clin. Immunol.* 101:778.
28. Takizawa, H., T. Ohtoshi, S. Kawasaki, T. Kohyama, M. Desaki, T. Kasama, K. Kobayashi, K. Nakahara, K. Yamamoto, K. Matsushima, et al. 1999. Diesel exhaust particles induce NF- $\kappa$ B activation in human bronchial epithelial cells in vitro: importance in cytokine transcription. *J. Clin. Allergy Immunol.* 162:4705.
29. Holgate, S. T., P. M. Lackie, D. E., Davies, W. R. Roche, and A. F. Walls. 1999. The bronchial epithelium as a key regulator of airway inflammation and remodeling in asthma. *Clin. Exp. Allergy* 29:90.
30. Boland, S., V. Bonvallot, T. Fournier, A. Baeza-Squiban, M. Aubier, and F. Marano. 2000. Mechanisms of GM-CSF increase by diesel exhaust particles in human airway epithelial cells. *Am. J. Physiol. Lung Cell Mol. Physiol.* 278:L25.
31. Steerenberg, P. A., J. A. Zonnenberg, J. A. Dormans, P. N. Joon, I. M. Wouters, L. van Bree, P. T. Scheepers, and H. Van Loveren. 1998. Diesel exhaust particles induced release of interleukin 6 and 8 by (primed) human bronchial epithelial cells (BEAS 2B) in vitro. *Exp. Lung Res.* 24:85.
32. Bayram, H., J. L. Devalia, R. J. Sapsford, T. Ohtoshi, Y. Miyabara, M. Sagai, and R. J. Davies. 1998. The effect of diesel exhaust particles on cell function and release of inflammatory mediators from human bronchial epithelial cells in vitro. *Am. J. Respir. Cell Mol. Biol.* 18:441.
33. Boland, S., A. Baeza-Squiban, T. Fournier, O. Houcine, M. C. Gendron, M. Chévrier, G. Jouvenot, A. Coste, M. Aubier, and F. Marano. 1999. Diesel exhaust particles are taken up by human airway epithelial cells in vitro and alter cytokine production. *Am. J. Physiol.* 276:L604.
34. Devalia, J. L., H. Bayram, C. Ruzsna, M. Calderón, R. J. Sapsford, M. A. Abdelaziz, J. Wang, and R. J. Davies. 1997. Mechanisms of pollution-induced airway disease: in vitro studies in the upper and lower airways. *Allergy* 52(Suppl. 38):45.
35. Wagner, J. G., S. J. Van Diken, J. A. Hotchkiss, and J. R. Harkema. 2001. Endotoxin enhancement of ozone-induced mucous cell metaplasia is neutrophil-dependent in rat nasal epithelium. *Toxicol. Sci.* 60:338.
36. Kutty, R. K., G. Kutty, C. N. Nagineni, Hooks, J. J., G. J. Chader, and B. Wiggert. 1994. RT-PCR assay for heme oxygenase-1 and heme oxygenase-2: a sensitive method to estimate cellular oxidative damage. *Ann. NY Acad. Sci.* 738:427.
37. Tietze, F. 1969. Enzymic method for quantitative determination of nanogram amounts of total and oxidized glutathione: applications to mammalian blood and other tissues. *Anal. Biochem.* 27:502.
38. Griffith, O. W. 1980. Determination of glutathione and glutathione disulfide using glutathione reductase and 2-vinylpyridine. *Anal. Biochem.* 106:207.
39. Bump, E. A., Y. C. Taylor, and J. M. Brown. 1983. Role of glutathione in the hypoxic cell cytotoxicity of misonidazole. *Cancer Res.* 43:997.
40. Yang, A. H., J. Gould-Kosta, and T. D. Oberley. 1987. In vitro growth and differentiation of human tubular cells on basement membrane substrate. *In Vitro Cell. Dev. Biol.* 23:34.
41. Mukaida, N., Y. Mahe, and K. Matsushima. 1990. Cooperative interaction of nuclear factor- $\kappa$ B- and cis-regulatory enhancer binding protein-like factor binding elements in activating the interleukin-8 gene by pro-inflammatory cytokines. *J. Biol. Chem.* 265:21128.
42. Mori, N., N. Mukaida, D. W. Ballard, K. Matsushima, and N. Yamamoto. 1998. Human T-cell leukemia virus type I tax transactivates human interleukin 8 gene through acting concurrently on AP-1 and nuclear factor- $\kappa$ B-like sites. *Cancer Res.* 58:3993.
43. Coppola, S., and L. Ghibelli. 2000. GSH extrusion and the mitochondrial pathway of apoptotic signaling. *Biochem. Soc. Trans.* 28:56-61.
44. Rahman, I., and W. MacNee. 2000. Regulation of redox glutathione levels and gene transcription in lung inflammation: therapeutic approaches. *Free Radical Biol. Med.* 28:1405.
45. Rahman, I., and W. MacNee. 2000. Oxidative stress and regulation of glutathione in lung inflammation. *Eur. Respir. J.* 16:534.
46. Rahman, I. 1999. Inflammation and the regulation of glutathione level in lung epithelial cells. *Antioxid. Redox. Signalling* 1:425.
47. Prester, T., P. Talalay, J. Alam, Y. I. Ahn, P. J. Lee, and A. M. Choi. 1995. Parallel induction of heme oxygenase-1 and chemoprotective phase 2 enzymes by electrophiles and antioxidants: regulation by upstream antioxidant-responsive elements (ARE). *Mol. Med.* 1:827.
48. Maines, M. D. 1997. The heme oxygenase system: a regulator of second messenger gases. *Annu. Rev. Pharmacol. Toxicol.* 37:517.
49. Nightingale, J. A., R. Maggs, P. Cullinan, L. E. Donnelley, D. F. Rogers, R. Kinnersley, K. F. Chung, P. J. Barnes, M. Ashmore, and A. Newman-Taylor. 2000. Airway inflammation after controlled exposure to diesel exhaust particulates. *Am. J. Respir. Crit. Care Med.* 162:161.
50. Alam, J., D. Stewart, C. Touchard, S. Boinapally, A. M. Choi, and J. L. Cook. 1999. Nrf2, a cap'n'collar transcription factor, regulates induction of the heme oxygenase-1 gene. *J. Biol. Chem.* 274:26071.
51. Chan, K., and Y. W. Kan. 1999. Nrf2 is essential for protection against acute pulmonary injury in mice. *Proc. Natl. Acad. Sci. USA* 96:12731.
52. Sen, C., and L. Packer. 1996. Antioxidant and redox regulation of gene transcription. *FASEB J.* 10:709.
53. Lander, M. 1997. An essential role for free radicals and derived species in signal transduction. *FASEB J.* 11:118.
54. Segura-Aguilar, J., D. Metodiewa, and C. J. Welch. 1998. Metabolic activation of dopamine *o*-quinone to *o*-semiquinones by NADPH cytochrome P450 reductase may play an important role in oxidative stress and apoptotic effects. *Biochim. Biophys. Acta* 1381:1.
55. Lei, W., R. Yu, S. Mandelkar, and A. T. Kong. 1998. Induction of apoptosis and activation of interleukin 1 $\beta$ -converting enzyme/ced-3 protease (caspase-3) and c-Jun NH<sub>2</sub>-terminal kinase by benzo(a)pyrene. *Cancer Res.* 58:2102.
56. Cai, J., and D. P. Jones. 1998. Superoxide in apoptosis: mitochondrial generation triggered by cytochrome C loss. *J. Biol. Chem.* 273:11401.
57. Kroemer, G., B. Dallaporta, and M. Resche-Rigon. 1998. The mitochondrial death/life regulator in apoptosis and necrosis. *Annu. Rev. Physiol.* 60:619.
58. Zoratti, M., and I. Szabo. 1995. The mitochondrial permeability transition. *Biochim. Biophys. Acta* 1241:139.
59. Fernández-checa, J. C., C. Garcia-Ruiz, A. Colell, A. Morales, M. Mari, M. Miranda, and E. Ardite. 1998. Oxidative stress: role of mitochondria and protection by glutathione. *Biofactors* 8:7.
60. Izzotti, A., A. Camoirana, F. D'Agostini, S. Sciacca, F. De Naro Papa, C. F. Cesarone, and S. De Flora. 1996. Biomarker alterations produced in rat lung by intratracheal instillation of air particulate extracts and chemoprevention with oral *N*-acetyl-cysteine. *Cancer Res.* 56:1533.
61. Goldsmith, C. A., A. Imrich, H. Danaee, Y. Y. Ning, and L. Kobzik. 1998. Analysis of air pollution particulate-mediated oxidant stress in alveolar macrophages. *J. Toxicol. Environ. Health A* 54:529.
62. Jaiswal, A. K. 1994. Commentary: antioxidant response element. *Biochem. Pharmacol.* 48:439.
63. Choi, A. M. K., and J. Alam. 1996. Heme oxygenase-1: function, regulation, and implication of a novel stress-inducible protein in oxidant-induced lung injury. *Am. J. Respir. Cell Mol. Biol.* 15:9.
64. Yamada, N., M. Yamaya, S. Okinaga, K. Nakayama, K. Sekizawa, S. Shibahara, and H. Sasaki. 2000. Microsatellite polymorphism in the heme oxygenase-1 gene promoter is associated with susceptibility to emphysema. *Am. J. Hum. Genet.* 66:187.